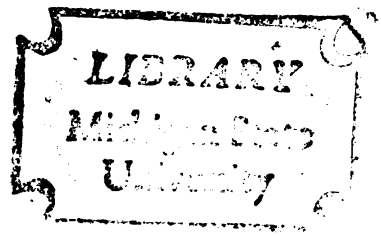

SIMULATION OF THE DYNAMICS OF A SOLAR COLLECTOR SYSTEM USING BOND GRAPHS

by

Syed Asif Nasar

A Thesis

Submitted to

Michigan State University

in partial fulfillment of the requirements

for the degree of

Master of Science

Department of Mechanical Engineering

1979

ABSTRACT

Simulation of the Dynamics of a
Solar Collector System Using Bond Graphs

by

Syed Asif Nasar

Using bond graphs, an effort has been made to study the dynamics of a solar collector system. The method is applied to a particular flat-plate solar collector typically used in residential heating and cooling.

The dynamic performance of the flat-plate solar collector predicted by the bond graph model was similar to that derived from the conventional model.

The conductive processes represented by the bond graph model are valid for all conditions but the convective model is only valid at low mass "flow" rate.

To Kamran, Rizwan and Sabuhi

"Dignity at all cost"

ACKNOWLEDGEMENTS

I would like to express my appreciation and thanks to my advisor, Professor Ronald C. Rosenberg for his guidance and support not only on this thesis but throughout my graduate and undergraduate programs.

Thanks also to many friendly people in the Department of Mechanical Engineering for making my stay at Michigan State University a worthwhile and enjoyable experience.

My humble thanks to my father, for his untiring effort in providing me with the best of everything; to my mother, for teaching me love and patience; and to both, for their continued love and prayers for me, without which this would not be possible.

My sincere appreciation to my sister and brother-in-law for putting up with me for six long years. And last but definitely not the least, my many thanks and love to my little sister, my "gurya" Sabuhi, for her encouragement, love and prayers, without which I could not have achieved my goals.

TABLE OF CONTENTS

LIST OF TABLES

LIST OF FIGURES

CHAPTER 1 INTRODUCTION

Renewed interest in solar energy has developed since 1973 as a result of increasing costs of energy from conventional resources and the problems of importing and extracting fuels that are acceptable from environmental standpoints. The engineering design of solar extraction processes presents unique problems, due to the intermittent and diffuse nature of the resource and the capital-intensive (high initial cost) nature of the processes.

Although solar energy may be considered a new or unconventional resource, it has been in use historically for several applications. Solar evaporation of salt brines to recover the salts has been practiced for many centuries, as has solar drying of agricultural products. Solar water heating is a standard method of providing domestic hot water in parts of Australia and Japan (1)[1] and small viable industries are based on the manufacture, sale and installation of solar water heating equipment in these countries.

1.1 Objectives

The purpose of this thesis is to investigate the feasibility of using a bond graph approach to study the dynamics of a solar collector system. The objective is threefold: (1) to derive a mathematical model of the solar collector using a bond graph, (2) to study the dynamics of a solar collector system once the mathematical model is derived, and (3) to consider the utility of the bond graph approach in the study of solar collector systems.

[1] Numbers in parentheses designate references.

It should be noted that this thesis does not attempt to be comprehensive, in that it concentrates on the solar collector rather than the use of solar energy for residential heating and cooling.

1.2 Organization

A description of the solar collector system is presented in Chapter 2. Using the bond graph techniques as the principal tools, the solar collector system was modeled. The mathematical model was also derived by the conventional approach.

In Chapter 3 the procedure used in simulating the operation of this system is outlined. This simulation involved the use of hourly weather bureau data from Madison, Wisconsin. The performance of solar collector systems is also discussed.

Chapter 4 presents conclusions and recommendations derived from this study.

1.3 Bond Graphs

A bond graph is a topological diagram, clearly representing any physical network. It was invented in the 1960's by H.M. Paynter (2) after intensive study and use of block diagrams. However, many users of bond graphs have brought them to their present state of utility. As an example of the present state of the art using the Enport program, the elements of a bond graph and their numerical values can be directly typed in a computer and the program will derive the system state equations and analyse it.

For those interested in bond graphs and bond graphs computer analysis, informative references are "System Dynamics: A Unified Approach" by Karnopp and Rosenberg (3), the ASME "Journal of Dynamic Systems, Measurement, and Control" (4), "Introduction to Bond Graphs and Their

Applications" by Thoma (5), and "A User's Guide to Enport-4" by Rosenberg (6). In addition, Karnopp has investigated the convective aspect of heat transfer in his papers titled "A Bond Graph Modeling Philosophy for Thermofluid Systems" (7) and "Pseudo Bond Graphs for Thermal Energy Transport" (8).

In a compact but general form a definition of the Bond Graph Language is also given in Appendix B.

1.4 Literature Survey

The study of solar energy for use in residential heating and cooling has been done on only a very limited basis. Previous work is more substantial in the area of solar energy use in providing service hot water. In the last twenty years, quite a few solar energy houses have been constructed.

For example, M.I.T. has been studying solar houses for a number of years and Engebretson (9) summarizes the operation of the fourth and last solar house for the years of 1959 and 1960. The performance of this house was felt to be satisfactory with no major problems encountered.

An experimental system which provides heating and cooling for a house in Tucson, Arizona, was studied by Bliss (10). This house and solar energy system is not the type that would prove economically feasible for widescale use, since its cost is quite large. However, as pointed out by the author, the house is constructed for the main purpose of studying the conversion and use of solar energy for residential heating and cooling.

Another variation of the solar energy home is presented by Thomason and Thomason (11, 12), one which uses a simple type of solar

collector and energy storage by means of a large water tank, which is surrounded by a layer of stones.

Most of the early work in the field of solar energy for residential use was summarized in a report of the proceedings of a symposium held in 1950 at M.I.T. (13). Collector models and system models presented at this symposium are still being used today.

One of the earlier computer studies of the dynamics of a solar collector system was made by Buchberg and Roulet (14). Equations modelling a solar energy system were used with hourly weather bureau data to accomplish the simulation.

One of the earlier references to solar heating and cooling was made by Lof (15) in 1955 in which he discussed the use of triethyl glycol for dehumidification of air. In a more recent paper Tybout and Lof (16) discuss the results of a computer simulation of house heating for various sites in the United States. Equations with eight design parameters were used to describe the system, and hourly weather bureau data were employed for use on a digital computer. Of the eight parameters studied, the effects of collector size, geographic location, building construction and number of glass covers on the collector were most significant.

Klein, Beckman and Duffie (17) made a computer study of a model in Albuquerque, New Mexico, for a solar heating and cooling system. The result was positive in the sense that an economical solar heating system could be designed by a simple graphical method requiring monthly average meteorological data.

In a report of the proceeding of a symposium held in 1977 at the Winter Annual Meeting of the American Society of Mechanical Engineers at

Atlanta, Georgia (18), the papers deal with three broad topics: analysis and experimental behaviour of heat transfer in solar collectors and in storage systems; experimental evaluation of complete solar systems; and computer analysis and simulation of complete solar systems. The volume gives a good overview of on-going work in these areas, and serves as both a reference and a survey.

CHAPTER 2 SOLAR COLLECTOR SYSTEM MODEL

2.1 Solar Energy System

The use of solar energy for providing heating, cooling and service hot water to a typical residence is illustrated in Figure 1 (19). The study of such a system is made possible by describing all of its components by mathematical models. In addition, a building mathematical model is also required to determine the heating and cooling loads encountered by a typical residence. This mathematical model can be derived either by using a bond graph approach or by conventional approach. In this study the bond graph approach is used to derive the mathematical model for the solar collector system.

The system, illustrated in Figure 1, includes a solar collector, an energy storage tank, a space heating system, a central air conditioner, a service hot water system and a main auxiliary heater.

The energy transfer medium for the system is water. This was chosen for simplicity since the variations in boiling points, specific heats and other properties of, mixtures containing various amounts of anti-freeze and anti-rust additives was beyond the scope of this research project. The system is a closed, pressurized system at 21 psia, which allows the water to reach 230^{o}F without boiling.

As mentioned earlier, this study is restricted to the consideration of thermal processes in which solar radiation is absorbed by a surface,the solar collector, and converted to the internal energy of the working fluid.

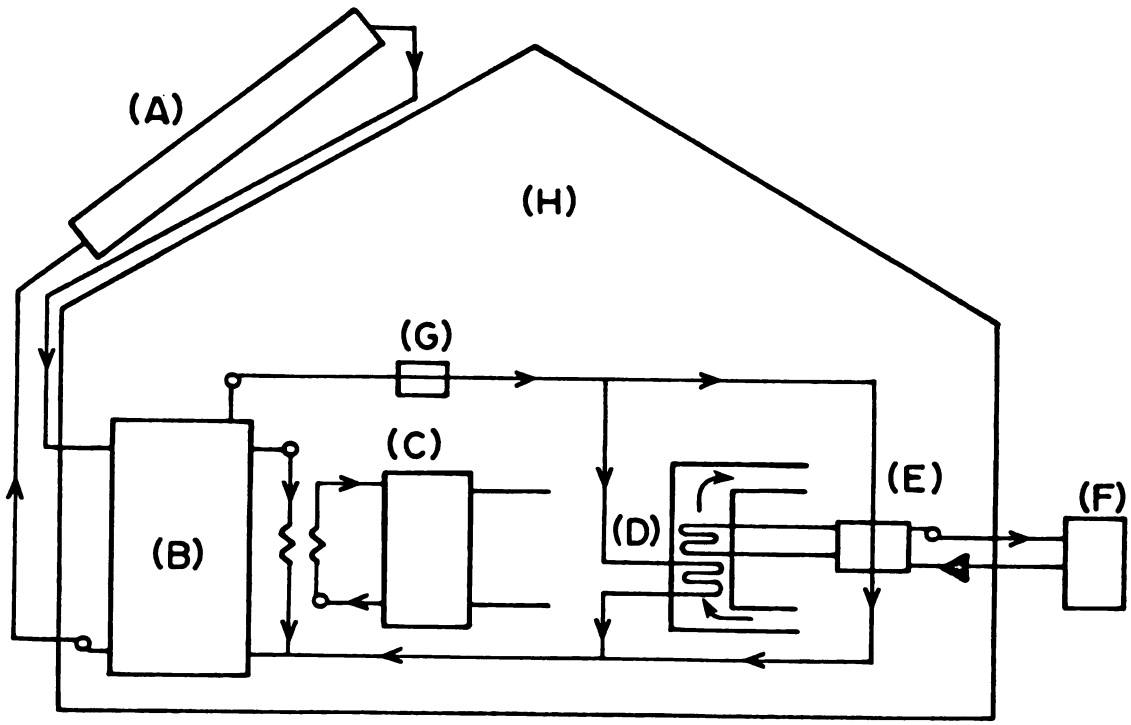

Figure 1. Solar Energy System and Residence*

(A) - Solar Collector, (B) - Energy Storage Tank,

(C) - Service Hot Water System, (D) - Air Heater,

(E) - Air Conditioner, (F) - Cooling Tower,

(G) - Main Auxiliary Heater, (H) - Residence

* Taken from (19), Figure 1

2.2 Details of the Solar Collector System

The solar collector is one essential item of equipment whose function is to transform the solar radiation incident on its surface into thermal energy of a working fluid which is transferred to the energy storage tank.

The collector is modelled with a "multi-node" capacitance (20, 21). Such a model is developed by considering the collector to consist of multiple nodes, each with a single temperature and capacitance. The nodes are positioned at a single glass cover, at the collector plate and at each of the four "lumps" of the fluid. The multi-node model can be extended to simulate the performance of flat plate collectors with more than one glass cover by the addition of a node at each cover.

The important parts of a typical flat-plate solar collector as shown in Figure 2 are: the "black" solar energy-absorbing surface, with means for transferring the absorbed energy to water; one transparent glass cover to shield solar radiation over the solar absorber surface in order to reduce convection and radiation losses to the atmosphere; and back insulation which causes the conduction and convection losses to be negligible.

Water is circulated through the collector by means of a pump whenever conditions are such that the value of the energy transferred to the working fluid is positive.

Keeping the cost in mind, realistically speaking, pump activation should occur when the value of the energy obtained is greater than the cost of operating the pump. However, I chose pump activation criterion to be a positive Qu because the main purpose of this research is to study the conversion and use of solar energy. Whatever reasonable

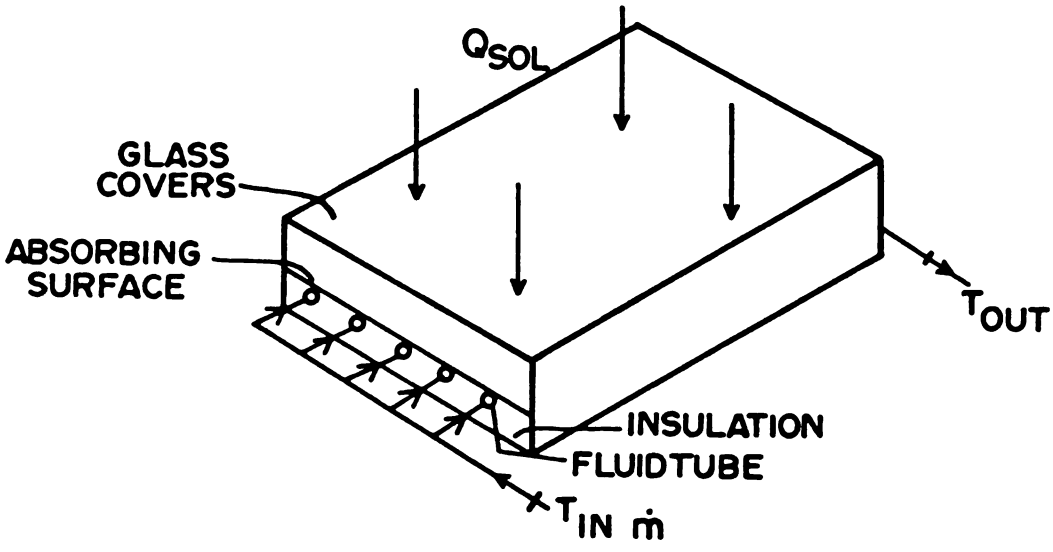

Figure 2. Solar Collector

criterion is used to activate the pump, this point is minor in comparison to the overall performance of the solar collector.

To prevent overpressurization of the closed system with water in the collector, the temperature of the exiting water from the collector is monitored such that whenever its value reaches 230°F an energy dissipation mechanism is activated. This simulated system allows the collector to get rid of the energy when it is operating at conditions which would cause an exiting temperature greater than 230°F. When operating at these overflow conditions the exiting temperature of the water is constant at its maximum value of 230°F.

Throughout this study the following assumptions are made:

The flow is steady state and incompressible with the parameter $\Delta M/M$ always less than one. The glass cover and the collector absorbing plate are uniform thermally speaking. Each "lump" of fluid is also uniform in its temperature. The temperature of sky is considered to be the same as temperature ambient. Only the beam radiation is considered and the black loss is assumed to be negligible.

2.3 Bond Graph Model

Bond graphs have been shown to be useful in the modelling of a wide variety of physical dynamic systems, but open systems in which several types of energy are transported across boundaries with mass flow have not been modelled as elegantly as fixed mass systems and their analogs. For the solar collector system a bond graph approach is outlined here which allows most of the conceptual and practical advantages of normal bond graph techniques to be retained for systems like this in which thermal energy transported by a flowing fluid is important.

The aim of the modeling procedure outlined below is to create reasonable lumped parameter models for performance prediction. Thus it is not possible to give firm rules for selecting the number and size of the lumps nor is it possible to say in advance whether the perfect and instantaneous mixing assumption is satisfactory. However, the model is at least rational in the sense of energy conservation.

The thermal network for the solar collector is shown in Figure 3. The loss from the bottom of the collector is assumed to be negligible. If the solar collector is considered without being subdivided into smaller segments, it could be represented as shown in Figure 4 by the word bond graph.

The effort and flow variables are temperature (T) and heat flow rate ($\dot{Q}$) respectively for the heat transfer model. When the variables T and $\dot{Q}$ are used for effort and flow, the product $T \cdot \dot{Q}$ has no special significance, since $\dot{Q}$ is already a power term. For this reason, the thermal bond graph is called a pseudo bond graph. In many respects, the thermal graphs resemble normal bond graphs, however. For example, the thermal state variable is Q, a displacement representing stored energy.

The most fundamental element in any bond graph is the bond itself or the part of ports which allow subsystems to be conjoined. Figure 5 shows the thermal bond graph model of the solar collector.

In Figure 5, the hydraulic part of the bond graph is not shown. This bond graph model would work very well for a purely conductive system. To allow for the convective nature of the heat removal from the collector plate, the hydraulic part of the model must be taken into account. Furthermore, in the model shown, the temperature of the water

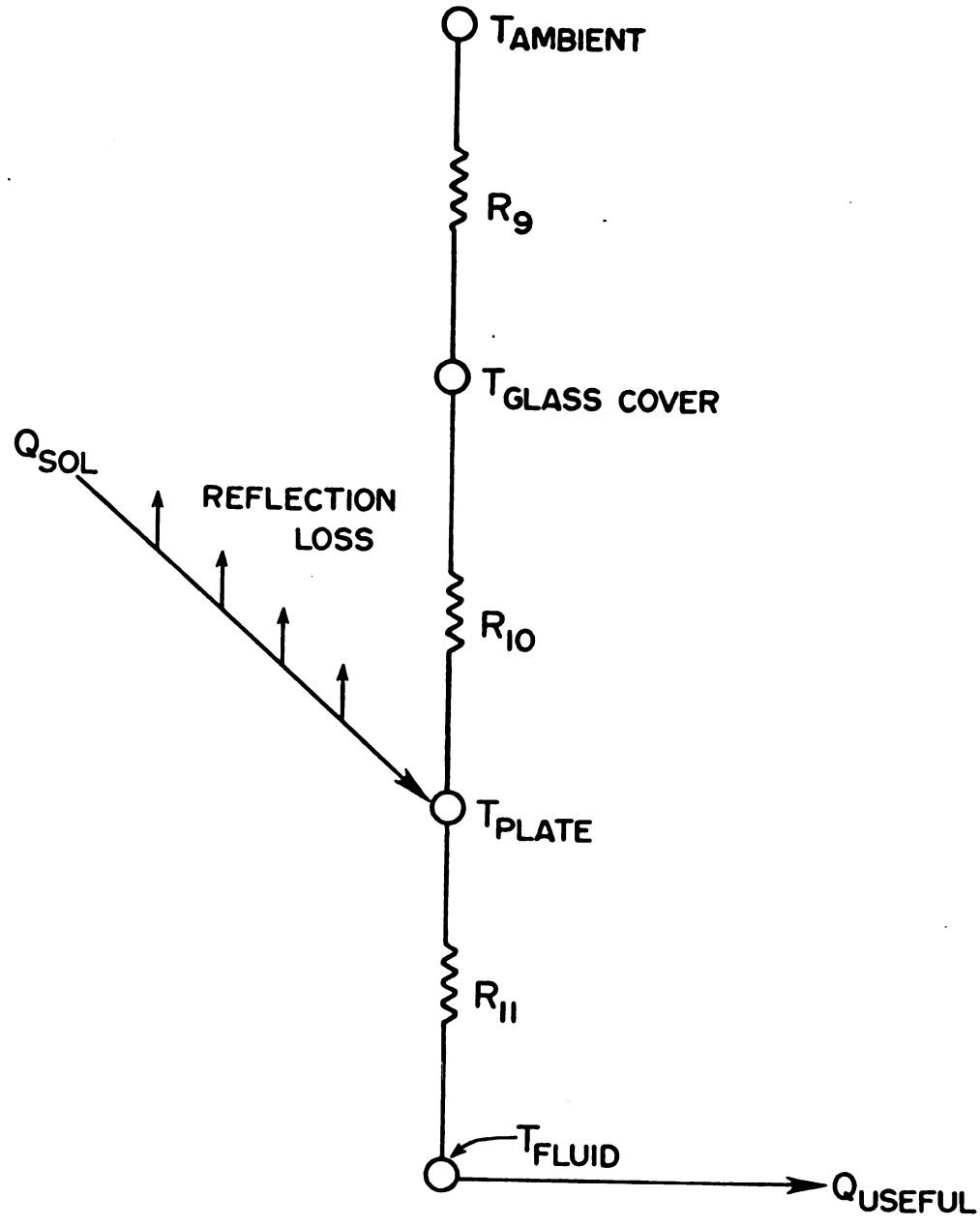

Figure 3. Thermal Network for Flat-Plate Solar Collector

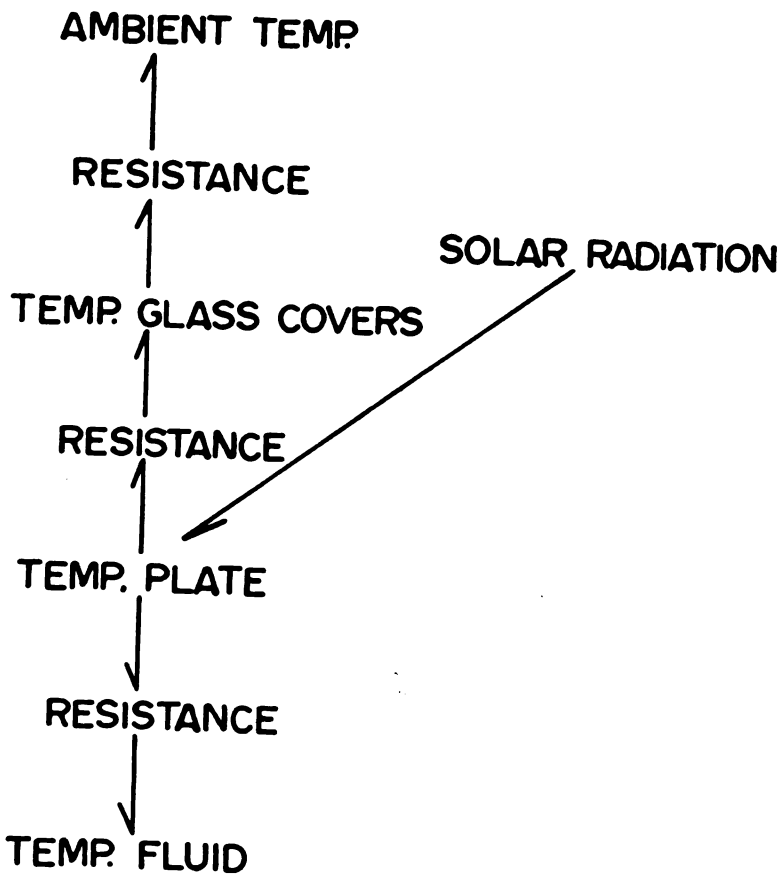

Figure 4. Word Bond Graph of Solar Collector

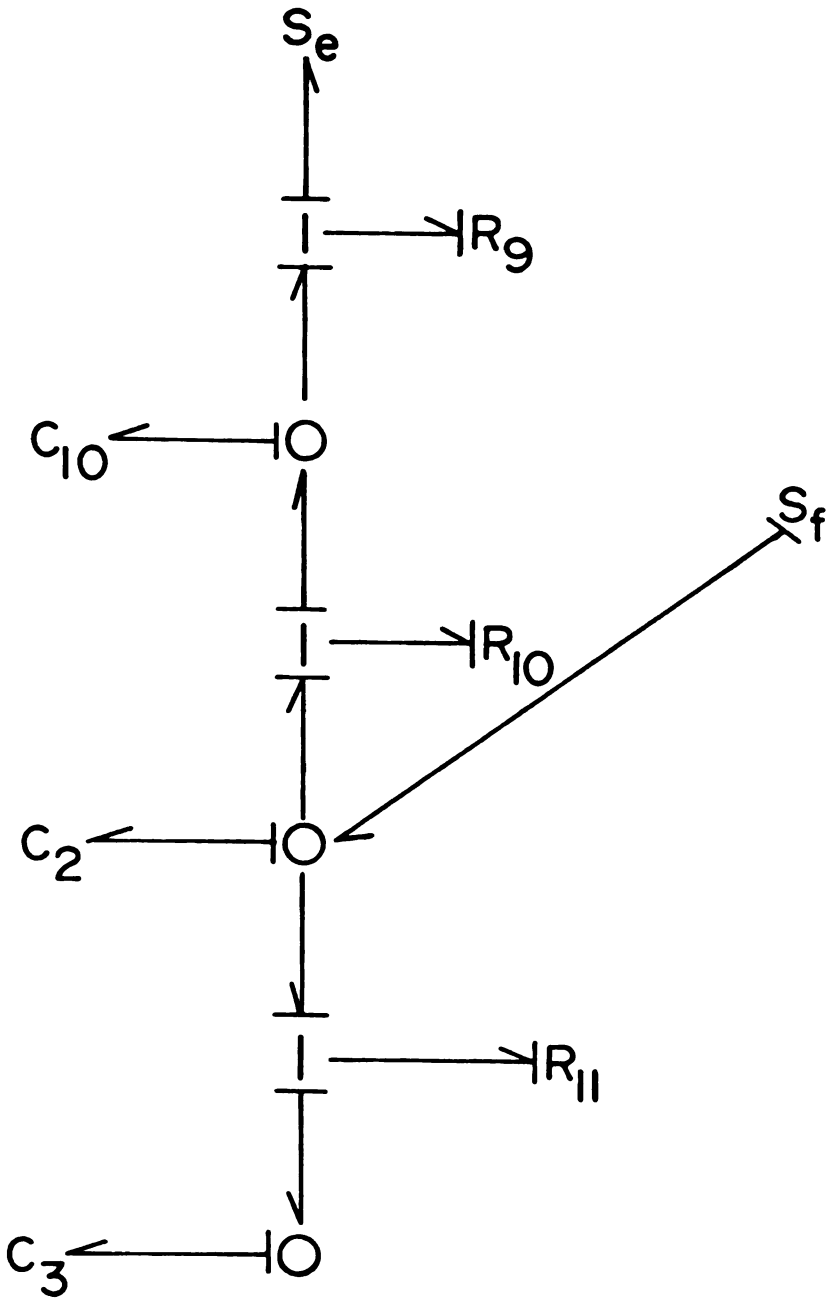

Figure 5. Bond Graph with Causality

throughout the entire length of the solar collector is taken to be the same. To improve on the idea of instantaneous mixing of water throughout the collector length and improve the overall prediction accuracy of the model a major reticulation is made.

As shown in Figure 6, the solar collector is subdivided into four segments. The bond graph model for the conductive path is not altered; it is the convective path of the system that is greatly altered. At this time there is no novel way to represent the heat transfer between a solid and a fluid in a bond graph (for those interested in further investigating this problem see references 7 and 8).

To incorporate the convective path of the solar collector, the system is divided into two major models. The first model in the bond graph language is represented by Figure 7.

Figure 7 represents the purely conductive path of the system. To analyze the conduction dynamics of the system, the bond graph of Figure 7 presents a straightforward model for deriving the system state equations by means of existing rules. Since there are six independent thermal energy variables associated with the bond graph of Figure 7, we will get six system state equations. The six system state equations are:

$$(MC_p)_g\dot{T}_1 = A_c[R_9(T_7-T_1)-R_{10}(T_1-T_2)] \tag{2.1}$$

$$(MC_p)_p\dot{T}_2=A_c[Q_{sol}-R_{11}(T_2-T_3)-R_{12}(T_2-T_4)-R_{13}(T_2-T_5)-R_{14}(T_2-T_6)+R_{10}(T_1-T_2)] \tag{2.2}$$

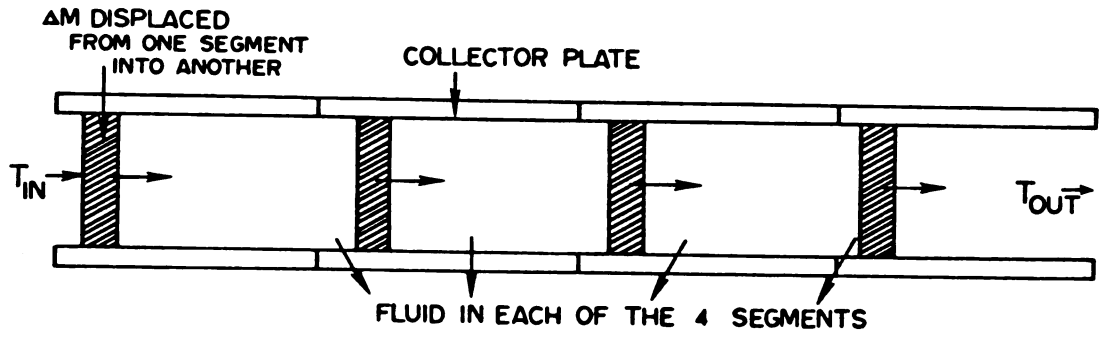

Figure 6. Solar Collector Subdivided into 4 Segment

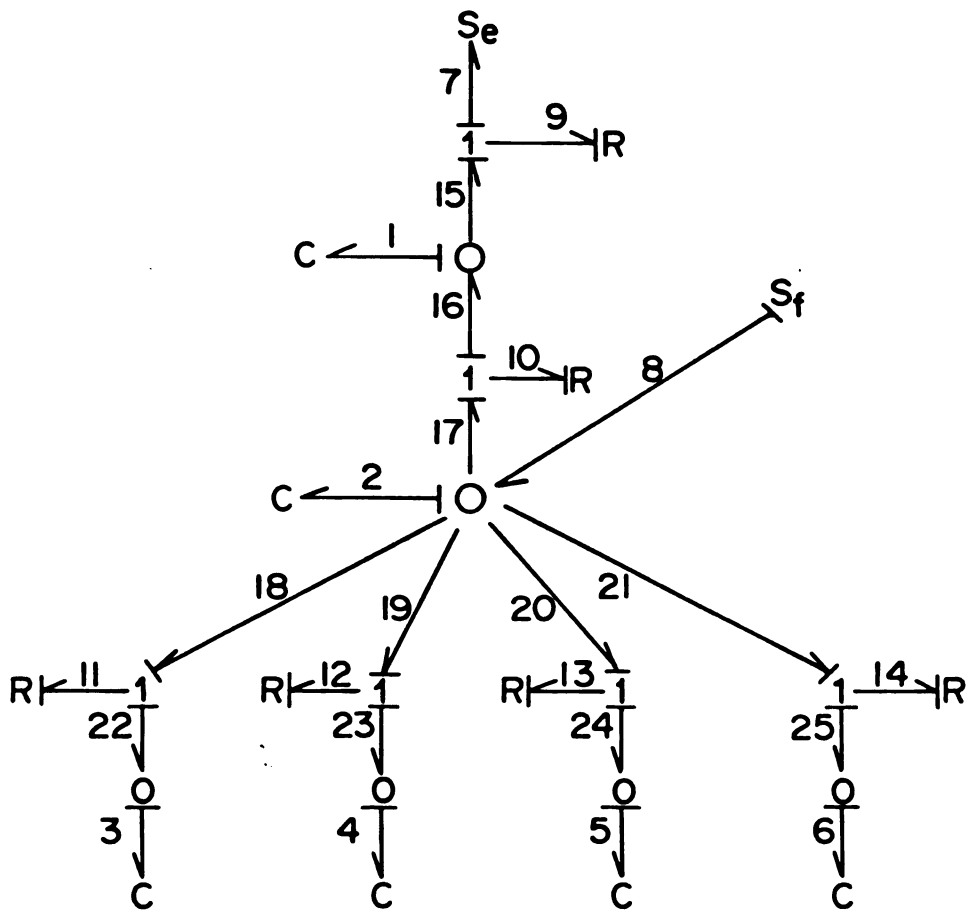

Figure 7. Bond Graph with Causality

$$(MC_p)_w \dot{T}_3 = (A_c/4) R_{11} (T_2 - T_3) \tag{2.3}$$

$$(MC_p)_w \dot{T}_4 = (A_c/4) R_{12} (T_2 - T_4) \tag{2.4}$$

$$(MC_p)_w \dot{T}_5 = (A_c/4) R_{13} (T_2 - T_5) \tag{2.5}$$

$$(MC_p)_w \dot{T}_6 = (A_c/4) R_{14} (T_2 - T_6) \tag{2.6}$$

where

$(MC_p)_g$ is the capacitance of the glass cover (BTU/F).

R_9 is the heat transfer coefficient (loss) between the ambient and the glass cover (BTU/hr-ft^2-F).

$\dot{T}_1 = \frac{dT_1}{dt}$, is temperature "flow" rate of the glass cover (F/hr).

T_7 is the ambient temperature (F).

T_1 is the temperature of the glass cover (F).

R_{10} is the heat transfer coefficient (loss) between the flat solar plate and the glass cover (BTU/hr-ft^2-F).

T_2 is the temperature of the flat solar collector plate (F).

$(MC_p)_p$ is the capacitance of the solar collector plate (BTU/F).

$\dot{T}_2 = \frac{dT_2}{dt}$.

Q_{sol} is the rate of the solar radiation intercepted by the solar collector plate (BTU/hr-ft^2).

R_i, i=11,12,13,14: heat transfer coefficient (loss) of cell i (BTU/hr-ft^2-F).

T_i, i=3,4,5,6: temperature of cell i (F).

$(MC_p)_w$ is the capacitance of water in each of the four cells (BTU/F).

T_6 is also the temperature of water exiting from the collector.

$\dot{T}_i = \frac{dT_i}{dt}$, i=3,4,5,6 (F/hr).

A_c=collector are (ft^2).

In order to get the solution of the six equations above we have to know the value of T_i, i=1,2,3,4,5,6. Since there are four unknowns due to the convective nature of heat transfer from the plate surface to the fluid, we must get four algebraic equations to find these unknowns.

Here we take a little deviation from the normal bond graph approach. As shown in Figure 8, each segment of the solar collector is numbered. In order to get the equation for the convective path, the following rules are followed.

Let the location of the fluid be represented by K and the time stage by i.

"Freeze i"; that is, there is no time advance. Then allow energy to redistribute itself by conduction thereby redistributing the temperature T_K,i. This would account for the mass flow rate ($\dot{M}$) effect instantaneously. Mass conservation is automatically satisfied for steady state fluid flow, since mass leaving K-1 cell enters K cell and mass leaving K cell enters K+1 cell. Also energy conservation is also satisfied if energy leaving K-1 cell enters K cell and energy leaving K cell enters K+1 cell. Since energy redistributes itself during each stage i, the "temperature" is also redistributed.

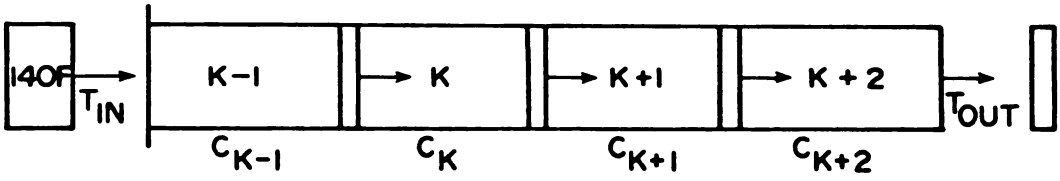

Figure 8. Convective Path Within the Solar Collector Tubes (Heat Removal Path)

An energy balance is made on each cell. In words the energy balance is written as:

> The new energy in cell K = (the energy already present in call K) + (the energy that enters cell K from cell K-1) - (the energy that leaves cell K and enters cell K+1).

In equation form the above could be expressed as:

$$\text{New } U_{K,i} = \text{Present } U_{K,i} + \Delta U_{K-1,i} - \Delta UK,i$$

where

$$\Delta U = \Delta M C_p T.$$

Once an energy balance has been made on a particular cell, the new temperature of that cell is determined immediately as:

$$C_p M T_{new} = \text{New U.}$$

Using the above technique the four algebraic equations for the convective path are found to be:

$$T_{new3} = T_3(1 - \frac{\Delta M}{M}) + \frac{\Delta M}{M} T_{in} \tag{2.7}$$

$$T_{new4} = T_4(1 - \frac{\Delta M}{M}) + \frac{\Delta M}{M} T3 \tag{2.8}$$

$$T_{new5} = T_5(1 - \frac{\Delta M}{M}) + \frac{\Delta M}{M} T4 \tag{2.9}$$

$$T_{new6} = T_6(1 - \frac{\Delta M}{M}) + \frac{\Delta M}{M} T5 \tag{2.10}$$

where

T_{newi}, i=3,4,5,6: new temperature of cell i(F).

T_i, i=3,4,5,6: Temperature of cell i before an energy balance was made (F).

M is the amount of water in cell (lbm).

ΔM is the amount of water "displaced" from each cell (lbm).

T_{in} is the inlet temperature of the fluid (F).

The set of ten equations derived above is simulated on a CDC 6500 digital computer to analyze the dynamic response of the flat-plate solar collector.

2.3.1 Improvement of the Convective Model

The methodology described to model the convective heat transfer, from the solar collector plate into the working fluid, could be improved by inserting a conductance effect on a common flow junction between pairs of common effort junctions representing the fluid "lumps". This is shown in the bond graph model of Figure 9. The conductance parameter is $\dot{M}C_p$, and increases with the mass flow rate. Activation of the upstream bond indicates that there is no direct flow effect. (For a discussion of activation see reference 3, page 30). The concise model shown in Figure 9 is possible because $\dot{M}C_p$ is constant for each "lump". Otherwise a more general two-port R must be used (see reference 8).

As illustrated in Figure 9, the bond graph model of Figure 7, after the necessary modifications,is now able to account for the mass

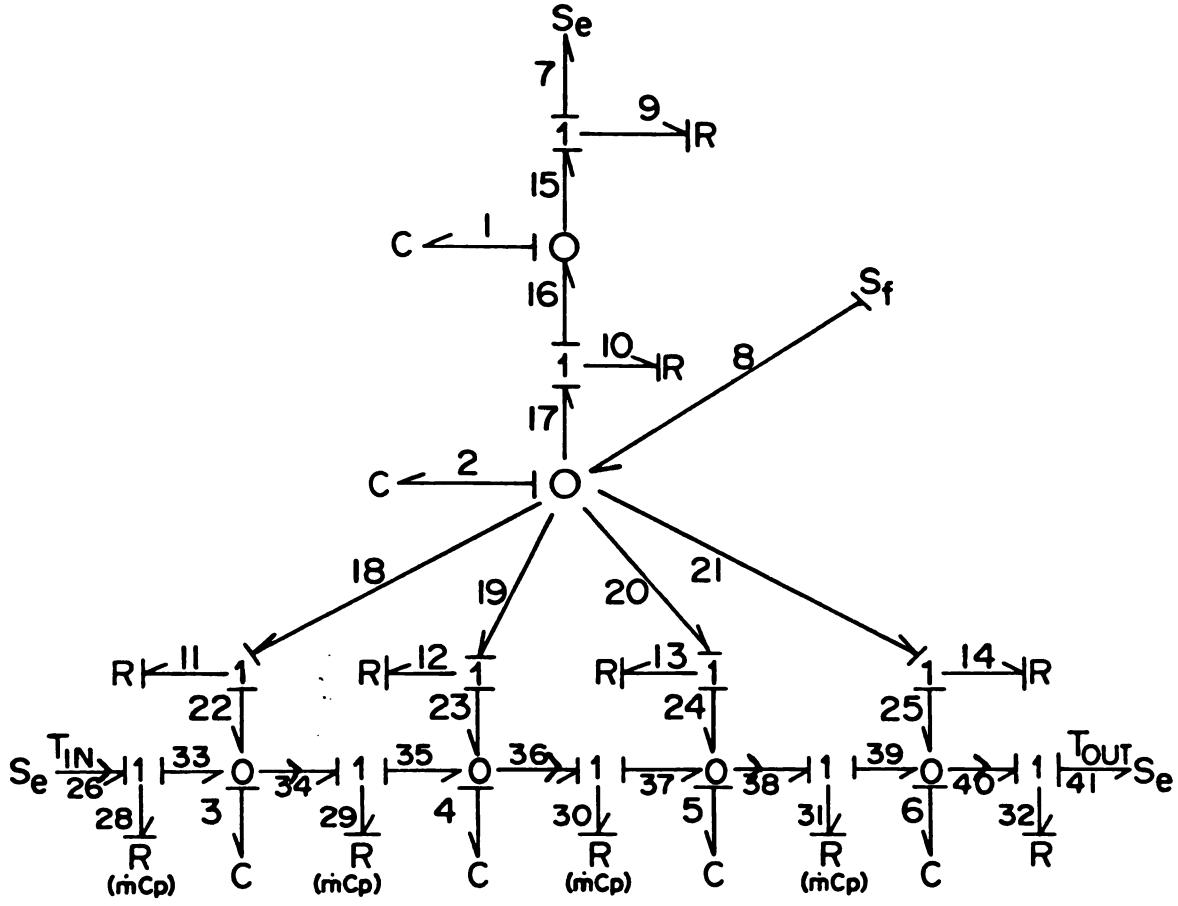

Figure 9. Bond Graph with Causality for Both Conductive and Convective Processes

flow effect of the fluid within the collector tube. By applying the existing rules to Figure 9, equation 2.3 to equation 2.6 could be modified to include the convective heat transfer within the collector tube. The modified equations are:

$$(MC_p)_3\dot{T}_3=R_{28}(T_{in}-T_3)+R_{11}A_c(T_2-T_3) \tag{2.3.1}$$

$$(MC_p)_4\dot{T}_4=R_{29}(T_3-T_4)+R_{12}A_c(T_2-T_4) \tag{2.4.1}$$

$$(MC_p)_5\dot{T}_5=R_{30}(T_4-T_5)+R_{13}A_c(T_2-T_5) \tag{2.5.1}$$

$$(MC_p)_6\dot{T}_6=R_{31}(T_5-T_6)+R_{14}A_c(T_2-T_6) \tag{2.6.1}$$

where

$(MC_p)_i$, i=3,4,5,6: Capacitance of water in each of the four "lump" (BTU/F).

T_i, $= \frac{dT_i}{dt}$, i=3,4,5,6 (F/hr).

T_{in} = inlet temperature of the fluid (F).

T_{out} = outlet temperature of the fluid (F).

$R_i=\dot{M}C_p$, i=28,29,30,31,32 (BTU/hr^{0}F).

$\dot{M}$ = mass flow rate (lbm/hr).

C_p = specific heat of fluid (BTU/lbm-F).

$R_i=U_i$, i=11,12,13,14, is the heat transfer coefficient (loss) of cell i (BTU/hr-ft^2-F).

A_c is the collector area (ft^2).

It should be noted that the conduction loss between the two adjacent "cells" is so small, that for all practical purposes it should be neglected without having any serious effect on the prediction of the dynamic performance of the collector.

Equations 2.1 and 2.2 together with equation 2.3.1 to equation 2.6.1 are the six state equations derived from the bond graph model of Figure 9. These state equations represent a complete mathematical model for the dynamic performance of the solar collector and could be programmed in a digital computer to predict the system performance.

2.4 Conventional Approach

Conventionally the solar collector is modelled with zero thermal capacitance. A zero capacitance model is one in which the effects of thermal capacitance on collector performance are neglected. The collector is considered to be in equilibrium with its environment at any instant of time.

The energy absorbed by the solar collector is determined by the following relation:

$$H_R = H_S R_T T_g \alpha p \tag{2.11}$$

where

H_R is the energy absorbed by the solar collector (BTU/hr-ft^2).

H_S is the radiation on a horizontal surface (BTU/hr-ft^2).

R_T is the correction factor which converts the radiation on a horizontal surface to that on the inclined surface of the collector. This factor is a function of the latitude, declination, time of day, tilt angle of and the azimuth angle.

T_g is the transmittance of the glass cover over the collector plate as a function of the angle of incidence of the solar radiation.

αp is the absorbtivity of the blackened collector plate as a function of the angle of incidence.

Not all the absorbed energy, however, is transferred to the working fluid. A small amount of the absorbed energy is lost to the

surroundings with the remaining energy transferred to the water circulating through the tubes which are attached to the collector plate. The relationship between the absorbed energy, losses to the surroundings and the useful energy is given by:

$$Q_u = FAc[H_R - U_L(T_{in} - T_{amb})] \tag{2.12}$$

where

Q_u is the rate of energy transfer to the water circulating through the collector (BTU/hr).

F is an efficiency factor that accounts for heat losses occurring at a mean temperature greater than the entering water temperature.

Ac is the collector area (ft^2).

U_L is the heat loss coefficient for heat losses to the surroundings (BTU/hr-ft^2F).

T_{in} is the temperature of water entering the collector (F).

T_{amb} is the ambient air temperature (F).

From a purely convective point of view the rate of energy addition to the water is also described by an energy balance.

$$Q_u = \dot{M}C_p(T_{out} - T_{in}) \tag{2.13}$$

where

$\dot{M}$ is the mass flow rate of the water through the collector (lbm/hr).

C_p is the specific heat of water (BTU/lbm-F).

T_{out} is the temperature of the water coming out of the collector (F).

Once H_R is calculated from equation (2.11), its value could be used in equation (2.12) to get Q_u. From equation (2.13) with the value of Q_u already known T_{out} could be calculated.

CHAPTER 3 Dynamic Performance of the Solar Collector System

3.1 Simulation Procedure

The mathematical equations described in Chapter 2, section 2.3, were programmed on a digital computer to study the dynamics of a flat-plate solar collector.

The Euler method of integration was used to perform the integration of all differential equations. The integration interval (Δt) was picked to be 0.001 of an hour. The value of $\Delta M/M$ must always be less than 1 for the system to be stable.

The program goes through three loops (see Figure 10). The first loop allows the distribution of temperature due to conduction. On the completion of the first loop which accounts for 0.005 of an hour, the temperature of the fluid within the cell is adjusted for the convective process, that is, for the mass flow rate effect.

On completion of the second loop which accounts for 0.05 of an hour the temperature, t_i, i=1,2,3,4,5,6 for the conductive process and the subsequent adjusted temperatures for the convective process is printed.

On completion of the third loop the program has accounted for all the data for that hour and is now ready for a new set of data for the next hour. The data available to this program is the hourly weather bureau data. This program is constructed such that the system can be operated in any location by providing the appropriate weather bureau data for that site.

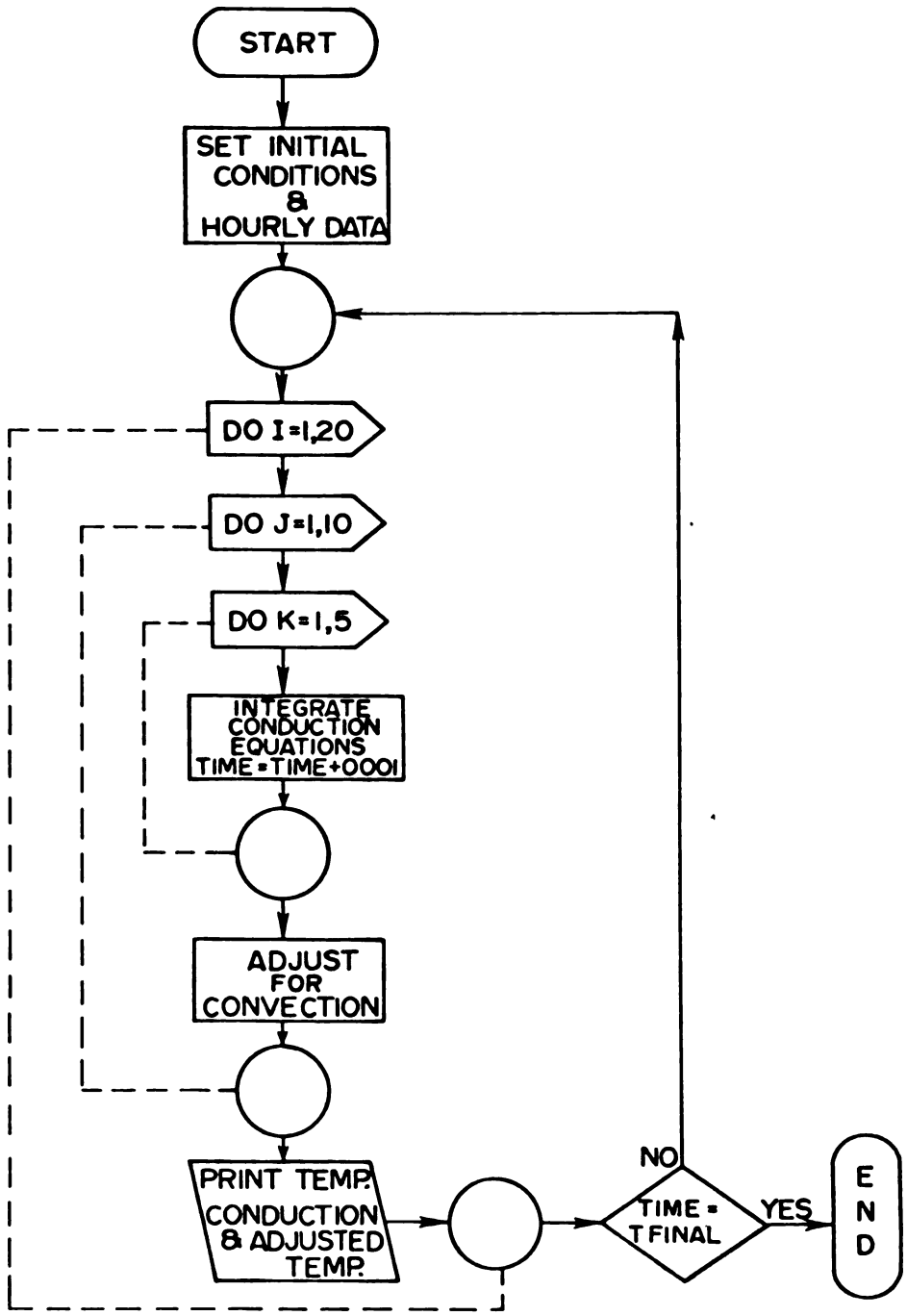

Figure 10. A Simple Flow Chart

Incidently, the bond graph of Figure 7 could be directly fed into the computer by using the Enport program. The output would be the equations and the dynamics of the conductive process.

3.2 Simulation Studies

The performance of the solar collector system was studied for the site of Madison, Wisconsin, using hourly weather bureau data. This site was chosen because the performance evaluation of the solar collector was available along with various data by means of the conventional approach.

Since the purpose of this study was to see whether it is feasible to use bond graphs as a modelling tool, the output of the bond graph model was compared to the output obtained from conventional models for a one-day cycle. No optimization was attempted.

Table 1 provides values and definitions for the main parameters used in the study. These values and values for many other parameters were either available with the problem or calculated by the authors of reference 1.

For each hour of the study the correction factor R was calculated for beam (specular) radiation only.

The error resulting from neglecting the diffuse radiation is not of major concern, since we are seeking validation of the basic modeling approach. However, the diffused radiation could easily be included in the model by adding a resistance between $T_{sky}(=T_{amb})$ and T_{plate} parallel to R_{10} of Figure 3. Also the correction factor R is calculated for the midpoints of the hours studied.

TABLE 1

Main Parameters

Parameter	Value	Comments
Collector Tilt	55 degrees	angle between plane of collector and horizontal
$\dot{M}$	158-59 lbm/hr	mass flow rate of water through collector
R9	5.20 BTU/hr-ft^2-F	heat loss coefficient from glass cover to ambient air
R10	1.64 BTU/hr-ft^2-F	sum of the convection and radiation coefficients from the collector plate to the glass cover
R11=R12=R13=R14	6.87 BTU/hr-ft^2-F	heat transfer coefficient from the water to the collector plate for each cell
$(C_pM)_g$	2.19 BTU/F	capacitance of the glass cover
$(C_pM)_p$	3.23 BTU/F	capacitance of the collector plate
$(C_pM)_w$	1.13 BTU/F	capacitance of water in each cell
Delta M	0.79 lbm	amount of water allowed to enter the solar collector at every .005 of an hour
Full M	1.132 lbm	amount of water present in each cell of the solar collector at every instance
NG	1	number of glass covers on collector
A_c	21.52 ft^2	collector area
T_{in}	140^{o}F	temperature of water entering the solar collector is constant
$T\alpha$	0.84	the transmittance absorptance product of this cover and absorber plate system

3.3 Results and Performance Evaluation

The performance of the flat-plate solar collector for one day selected from the month of January is presented in Table II and illustrated in Figure 11.

Figure 11 compares the result of this study with the one available in reference 1. As illustrated the performance of the flat plat solar collector using the bond graph appraoch tends to be very close to that of the conventional approach.

The small discrepancy between the two results could be attributed to various factors. One such factor is that the data available for various heat transfer coefficients is highly questionable. The authors of reference 1 admit that these values are simply crude estimations.

The difference in the two results may be attributed to these two major factors:

First not all the data was available with the original problem.

The values of R_9, R_{10}, R_{11} were not available with the problem. It was estimated by the authors and they admit that these were crude estimations.

The higher the value of the heat transfer coefficients (u), the less the loss. The value of u given in the problem is 1.409 BTU/hr-ft^2-F where as the value used in the bond graph model is 1.247 BTU/hr-ft^2-F.

It is this difference in the value of overall heat transfer coefficients that has caused the slight difference in the two calculations.

Furthermore the conventional model is a zero-capacitance model, in which the effects of thermal capacitance on the collector performance are neglected. The collector is considered to be in equilibrium with

TABLE II

Time (HR)	T_{AMB} (F)	S BUT/hr	T_{out} (calculated) (F)	Qusefull (calculated) (BTU/hr)	Efficiency
8	-	-	-	-	-
9	32.0	1733.22	136.14	0.00	0.00
10	35.6	2790.93	139.98	0.00	0.00
11	39.2	4278.61	145.25	840.14	0.196
12	50.0	5998.27	151.94	1910.07	0.318
13	50.0	6155.15	152.46	1993.62	0.324
14	46.4	5438.75	149.76	1560.76	0.287
15	46.6	4415.04	146.35	1015.55	0.230
16	42.8	2893.36	140.96	153.80	.053

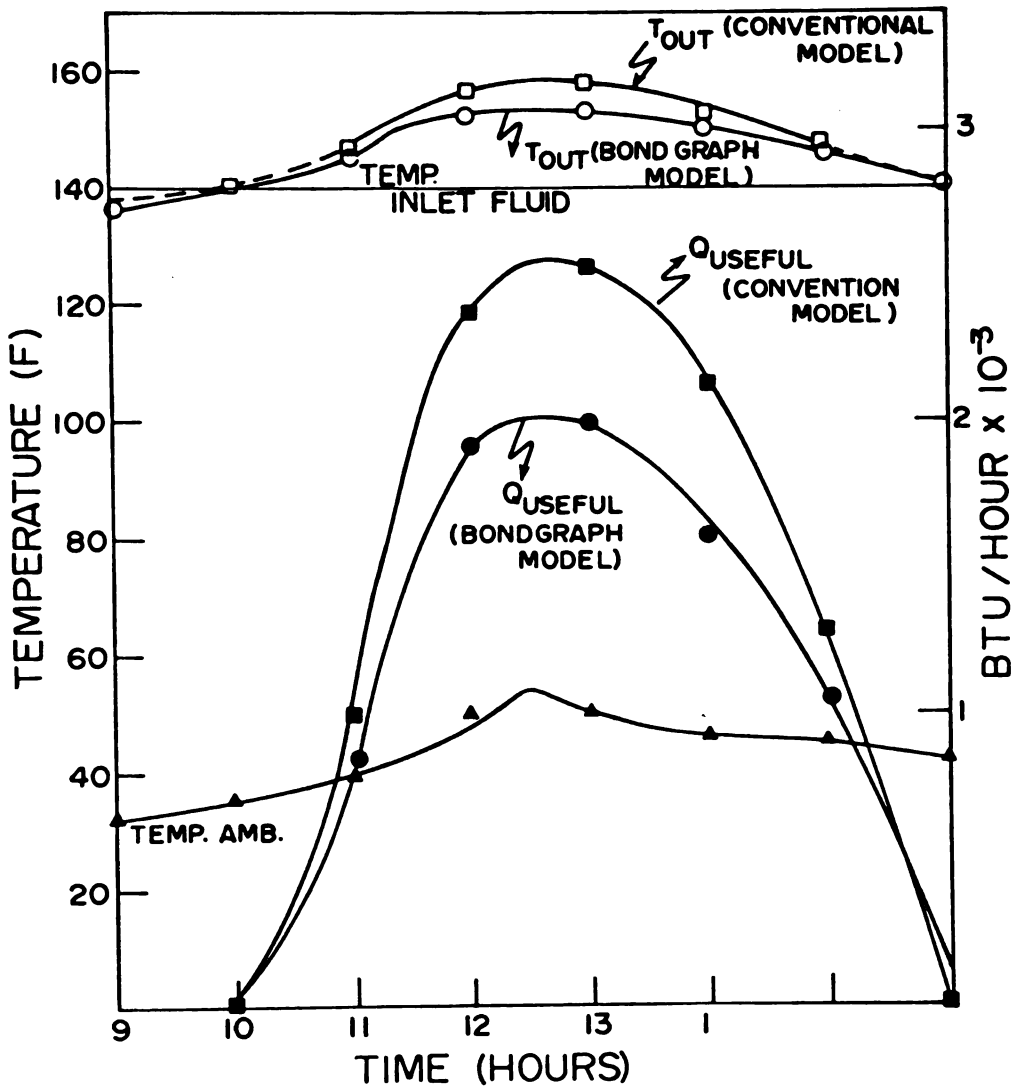

Figure 11. Comparison of Results

* The result of the conventional model is taken from reference (1)

its environment at any instant of time, whereas the bond graph model accounts for capacitance effects by dividing the collector into number of isothermal segments or nodes. Thus there is a slight difference in temperature at each node of the "multi-node" model.

Also the real advantage of this model would be more prominent in a larger system. The idea of modeling the whole system into lumps deals with the philosophy that for a larger system the instantaneous mixing effect is not reasonable and as such it should be modelled by smaller lumps. The system studied here was much too small for such a study to have any significant impact.

The efficiency of utilizing available solar energy for every hour studied is plotted in Figure 12. The overall efficiency of the solar collector for this study is 23%.

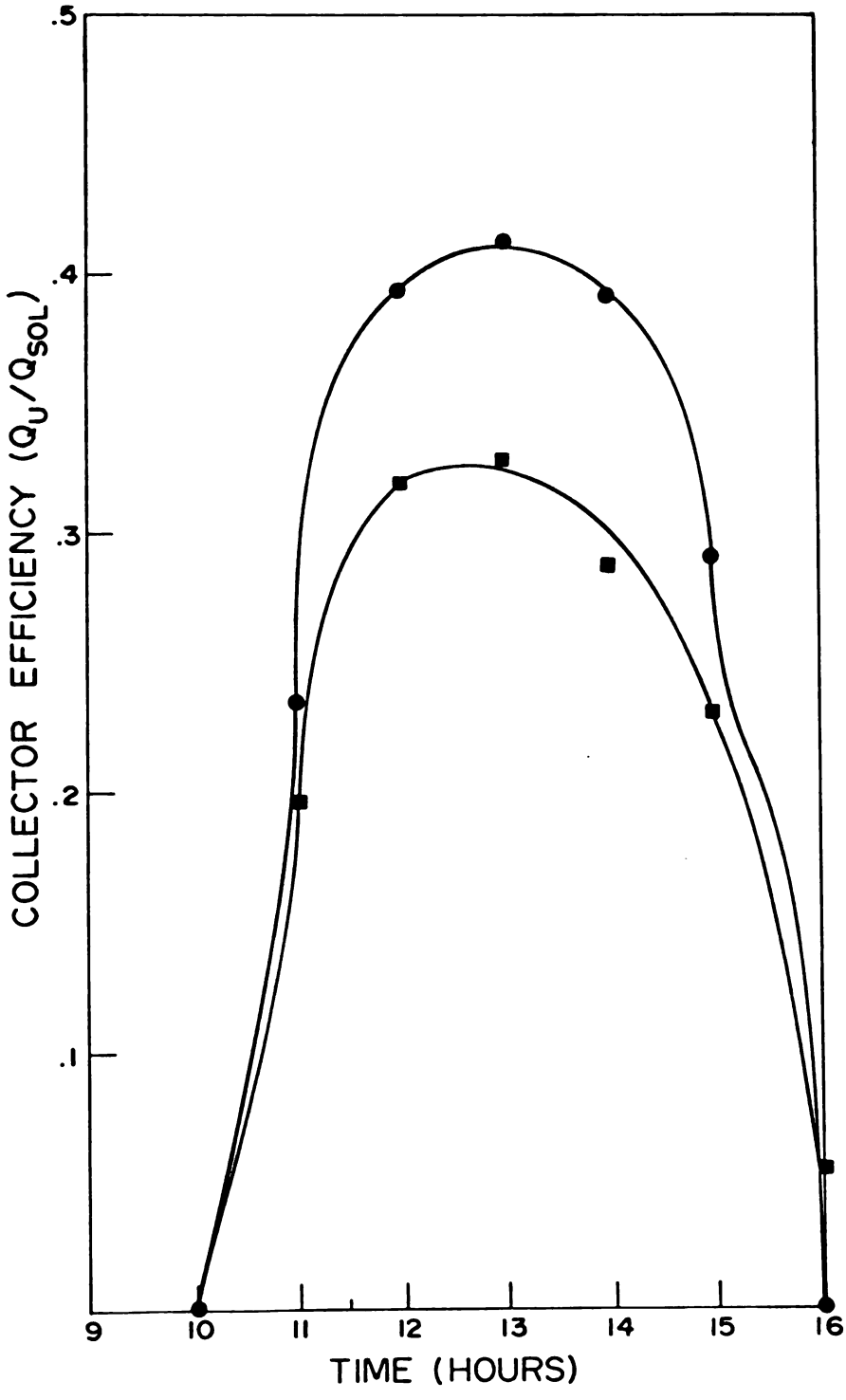

Figure 12. Collector Efficiency vs Time

CHAPTER 4 Conclusions and Recommendations

4.1 Utility of Bond Graphs for Modeling and Simulation

The three objectives of this research were (1) to derive a mathematical model of the flat-plate solar collector using bond graphs, (2) to study the dynamics of a flat-plate solar collector system once the mathematical model was derived, and (3) to consider the utility of the bond graph approach in the study of the flat-plate solar collector system.

The first objective was accomplished by lumping the thermal capacitance effects of each of the components of the flat-plate solar collector into a separate node, and then representing each node by bond graphs.

The bond graph approach as a modeling tool has a reasonable amount of versatility with respect to the study of the dynamics of a flat-plate solar collector irrespective of the model chosen. That is, by removing the "C"-element from the bond graph of Figure 7, the thermal capacitance effect would be eliminated. Consequently, the present approach could easily incorporate studies of the flat-plate solar collector without any major change to the conductive model. However, one of the major advantages of the present approach is its ability to study a wide range of possible "hook-ups" of the components to obtain the models not only of the flat-plate solar collector but many other, more complete systems, which have been used and proposed for solar energy use, including the entire building.

4.2 Solar Collector Models

The flat plate solar collector studied in this project could be improved for better dynamic performance by making certain changes in its design. One such change would be the addition of one more glass cover. This would minimize the losses caused by both convective and radiative processes. The back losses would be minimized if the temperature and the capacitance effect of the bottom insulation is included in the model.

For better performance of the collector, the tube spacing within the collector should be reduced from its present 6 inch center to center spacing.

Consideration should be given to low temperature operation. If the system operates in low temperate climates a freezing problem exists and the system must either be drained or anti-freeze must be added. Other types of weather problems exist. The system must be able to withstand wind loads, rain and hail. The collector must be designed so that snow does not interfere with winter time operation. All these could be readily included in the present model. This shows the strength and the versatility of the bond graph model.

4.3 Next Steps

Since this is the first such study of its kind, the bond graph model representing the solar collector leaves much to be desired.

One of the first things to do to increase the usefulness of bond graphs as a modeling tool is to improve the model for the convective processes. One way this might be done is by treating MC_p (mass flow rate times the specific heat of the fluid flowing through the

collector) as resistance, R, representing loss effects from the collector plate into the fluid passing through the collector tube.

Once this is done, the next step would be to model each of the components involved in the solar energy residential heating and cooling. Once the components are represented successfully, they should be "hooked-up" in the right order to describe the entire system. The bond graph should be used directly by the computer in order to study the collector performance. To achieve this, the Enport program must be able to handle a larger and more complex set of system models than its current capabilities allow.

REFERENCES

1. Duffie, J.A. and Beckman, W.A. Solar Energy Thermal Processes. New York: Wiley and Sons, 1974.

2. Dixhoorn, J.J. Van, and Evans, F.J. (eds) Physical Structure in Systems Theory. London: Academic Press, 1974.

3. Karnopp, D.C. and Rosenberg, R.C. System Dynamics: A Unified Approach. New York, Wiley and Sons, 1975

4. ASME, Journal of Dynamic Systems, Measurements, and Control. Sept. 1972.

5. Thoma, J.U. Introduction to Bond Graphs and Their Applications. Oxford: Pergamon Press, 1975.

6. Rosenberg, R.C. A User's Guide to Enport-4. New York: Wiley and Sons, 1974.

7. ASME, Journal of Dynamic Systems, Measurements, and Control. March 1978.

8. Karnopp, D.C. Pseudo Bond Graphs for Thermal Energy Transport. Contact the author.

9. Space Heating with Solar Energy. Proceedings of a Course Symposium, M.I.T., 1954.

10. Bliss, R.W. The Performance of an Experimental System Using Solar Energy for Heating and Night Radiation for Cooling a Building. Paper presented at U.N. Conference on New Sources of Energy, 1964.

11. Thomason, H.E. Solar Space Heating, Water Heating, Cooling in the Thomason House. Proceedings of the Conference on New Sources of Energy, August 1961, Vol. 5.

12. Thomason, H.E. and Thomason, H.J.L., Jr. Solar Houses/Heating and Cooling Progress Report. Solar Energy, Vol. 15, No. 1, May 1973.

13. Space Heating with Solar Energy. Proceedings of a Course Symposium, M.I.T., 1954.

14. Buchberg, H. and Roulet, J.R. Simulation and Optimization of Solar Collection and Storage for House Heating. Solar Energy, Vol. 12, No. 1, Sept. 1968.

15. Lof, G.O.G. House Heating and Cooling with Solar Energy. Paper in Solar Energy Research, University of Wisconsin Proceedings, 1955.

16. Tybout, R.A. and Lof, G.O.G. Cost of House Heating with Solar Energy. Solar Energy, Vol. 14, No. 3, Feb. 1973.

17. Klein, S.A., Beckman, W.A. and Duffie, J.A. A Design Procedure for Solar Heating Systems. Solar Energy, Vol. 18, No. 4, Nov. 1975.

18. ASME, Heat Transfer in Solar Energy Systems. Proceedings of the Winter Annual Meeting of the American Society of Mechanical Engineers, Atlanta, Georgia, Nov. - Dec. 1977.

19. Butz, L.W. Use of Solar Energy for Residential Heating and Cooling. M.S. Thesis in Mechanical Engineering, Madison, University of Wisconsin, 1973.

20. Close, D.J. A Design Approach for Solar Processes. Solar Energy, Vol. 11, 1967.

21. Klein, S.A., Duffie, J.A. and Beckman, W.A. Transient Considerations of Flat-Plate Solar Collectors. ASME, Journal of Engineering for Power, April 1974.

APPENDICES

APPENDIX A

Glossary of Terms

Glossary

A_c is the collector area (ft^2)

Beam Radiation is that solar radiation from the sun without change of direction.

$C_1=(MC_p)_g$, is the capacitance of the glass (BTU/F).

$C_2=(MC_p)_p$, is the capacitance of the solar plate (BTU/F).

$C_3=C_4=C_5=C_6=(MC_p)_w$, is the capacitance of water in each cell (BTU/hr).

Diffuse Radiation is that solar radiation received from the sun after its direction has been changed by reflection and scattering by the atmosphere.

H_R is the energy absorbed by the solar collector (BTU/hr-ft^2).

H_S is the radiation on a horizontal surface (BTU/hr-ft^2).

$\dot{M}$ is the mass flow rate (lbm/hr).

Q_{sol} is the solar radiation from the sun (BTU/hr-ft^2).

Q_u is the rate of energy transfer to the water circulating through the collector (BTU/hr).

$R_i=U_i$ is the heat transfer coefficient loss (BTU/hr-ft^2-F).

T_i is the temperatures (F).

R_T is the tile factor for beam radiation (see reference 1, page 49, equations 3.6.1 and 3.6.2 for detail).

APPENDIX B

A Definition of the Bond Graph Language

R. C. ROSENBERG

Associate Professor, Department of Mechanical Engineering, Michigan State University, East Lansing, Mich.

D. C. KARNOPP

Professor, Department of Mechanical Engineering, University of California, Davis, Calif.

A Definition of the Bond Graph Language

Introduction

THE purpose of this paper is to present the basic definitions of the bond graph language in a compact but general form. The language presented herein is a formal mathematical system of definitions and symbolism. The descriptive names are stated in terms related to energy and power, because that is the historical basis of the multiport concept.

It is important that the fundamental definitions of the language be standardized because an increasing number of people around the world are using and developing the bond graph language as a modeling tool in relation to multiport systems. A common set of reference definitions will be an aid to all in promoting ease of communication.

Some care has been taken from the start to construct definitions and notation which are helpful in communicating with digital computers through special programs, such as ENPORT [5].[1] It is hoped that any subsequent modifications and extensions to the language will give due consideration to this goal.

Principal sources of extended descriptions of the language and physical applications and interpretations will be found in Paynter [1], Karnopp and Rosenberg [2, 3], and Takahashi, et al. [4]. This paper is the most highly codified version of language definition, drawing as it does upon all previous efforts.

Basic Definitions

Multiport Elements, Ports, and Bonds. *Multiport elements* are the nodes of the graph, and are designated by alpha-numeric characters. They are referred to as elements, for convenience. For example, in Fig. 1(*a*) two multiport elements, 1 and *R*, are shown. *Ports* of a multiport element are designated by line segments incident on the element at one end. Ports are places where the element can interact with its environment.

For example, in Fig. 1(*b*) the 1 element has three ports and the *R* element has one port. We say that the 1 element is a 3-port, and the *R* element is a 1-port.

Bonds are formed when pairs of ports are joined. Thus bonds are connections between pairs of multiport elements.

For example, in Fig. 1(*c*) two ports have been joined, forming a bond between the 1 and the *R*.

Bond Graphs. A *bond graph* is a collection of multiport elements bonded together. In the general sense it is a linear graph whose nodes are multiport elements and whose branches are bonds.

A bond graph may have one part or several parts, may have no loops or several loops, and in general has the characteristics of any linear graph.

An example of a bond graph is given in Fig. 2. In part (*a*) a bond graph with seven elements and six bonds is shown. In part (*b*) the same graph has had its powers directed and bonds labeled.

A *bond graph fragment* is a bond graph not all of whose ports have been paired as bonds.

An example of a bond graph fragment is given in Fig. 1(*c*), which has one bond and two open, or unconnected, ports.

Port Variables. Associated with a given port are three direct and three integral quantities.

Effort, $e(t)$, and *flow*, $f(t)$, are directly associated with a given port, and are called the port power variables. They are assumed to be scalar functions of an independent variable (t).

Power, $P(t)$, is found directly from the scalar product of effort and flow, as

$$P(t) = e(t) \cdot f(t).$$

The direction of positive power is indicated by a half-arrow on the bond.

Momentum, $p(t)$, and *displacement*, $q(t)$, are related to the effort and flow at a port by integral relations. That is,

[1] Numbers in brackets designate References at end of paper.

Contributed by the Automatic Control Division for publication (without presentation) in the JOURNAL OF DYNAMIC SYSTEMS, MEASUREMENT, AND CONTROL. Manuscript received at ASME Headquarters, May 9, 1972. Paper No. 72-Aut-T.

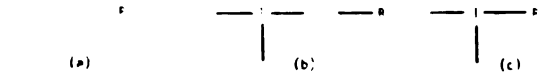

Fig. 1 Multiport elements, ports, and bonds: (a) two multiport elements; (b) the elements and their ports; (c) formation of a bond

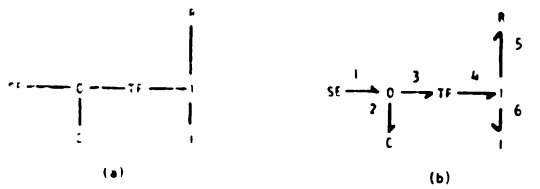

Fig. 2 An example of a bond graph: (a) a bond graph; (b) the bond graph with powers directed and bonds labeled

$$p(t) = p(t_0) + \int_{t_0}^{t} e(\lambda)d\lambda$$

and $q(t) = q(t_0) + \int_{t_0}^{t} f(\lambda)d\lambda$, respectively.

Momentum and displacement are sometimes referred to as energy variables.

Energy. $E(t)$, is related to the power at a port by

$$E(t) = E(t_0) + \int_{t_0}^{t} P(\lambda)d\lambda.$$

The quantity $E(t) - E(t_0)$ represents the net energy transferred through the port in the direction of the half-arrow (i.e., positive power) over the interval (t_0, t).

In common bond graph usage the effort and the flow are often shown explicitly next to the port (or bond). The power, displacement, momentum, and energy quantities are all implied.

Basic Multiport Elements. There are nine basic multiport elements, grouped into four categories according to their energy characteristics. These elements and their definitions are summarized in Fig. 3.

Sources.

Source of effort, written $SE\ e$, is defined by $e = e(t)$.

Source of flow, written $SF\ f$, is defined by $f = f(t)$.

Storages.

Capacitance, written $\overset{e}{\underset{f}{}}\ C$, is defined by

$$e = \Phi(q) \text{ and } q(t) = q(t_0) + \int_{t_0}^{t} f(\lambda)d\lambda.$$

That is, the effort is a static function of the displacement and the displacement is the time integral of the flow.

Inertance, written $\overset{e}{\underset{f}{}}\ I$, is defined by

$$f = \Phi(p) \text{ and } p(t) = p(t_0) + \int_{t_0}^{t} e(\lambda)d\lambda.$$

That is, the flow is a static function of the momentum and the momentum is the time integral of the effort.

Dissipation.

Resistance, written $\overset{e}{\underset{f}{}}\ R$, is defined by

$$\Phi(e, f) = 0.$$

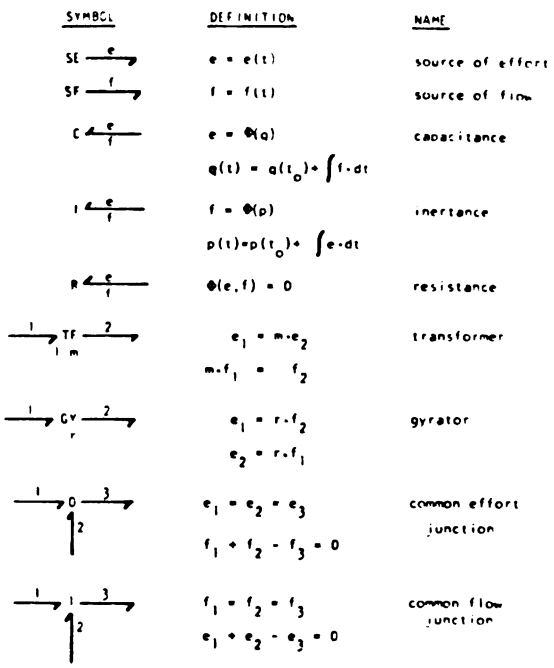

Fig. 3 Definitions of the basic multiport elements

That is, a static relation exists between the effort and flow at the port.

Junctions: 2-Port.

Transformer, written $\frac{e_1}{f_1}\ TF\ \frac{e_2}{f_2}$, is a linear 2-port element defined by

$$e_1 = m \cdot e_2$$

and $$m \cdot f_1 = f_2,$$

where m is the modulus.

Gyrator, written $\frac{e_1}{f_1}\ GY\ \frac{e_2}{f_2}$, is a linear 2-port element defined by

$$e_1 = r \cdot f_2$$

and $$e_2 = r \cdot f_1,$$

where r is the modulus.

Both the transformer and gyrator preserve power (i.e., $P_1 = P_2$ in each case shown), and they must each have two ports, so they are called essential 2-port junctions.

Junctions: 3-Port.

Common effort junction, written $\xrightarrow{1}\ 0\ \xrightarrow{3}$ with $\uparrow 2$

is a linear 3-port element defined by

$$e_1 = e_2 = e_3 \qquad \text{(common effort)}$$

and $$f_1 + f_2 - f_3 = 0. \qquad \text{(flow summation)}$$

Other names for this element are the *flow* junction and the

zero junction. *Common flow junction*, written 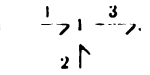 ,

is a linear 3-port element defined by

$$f_1 = f_2 = f_3 \qquad \text{(common flow)}$$

and $$e_1 + e_2 - e_3 = 0. \qquad \text{(effort summation)}$$

Other names for this element are the *effort* junction and the *one* junction.

Both the common effort junction and the common flow junction preserve power (i.e., the *net* power in is zero at all times), so they are called junctions. If the reference power directions are changed the signs on the summation relation must change accordingly.

Extended Definitions

Multiport Fields.

Storage Fields. *Multiport capacitances*, or *C-fields*, are written 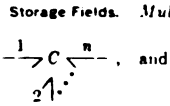 , and characterized by

$$e_i = \Phi_i(q_1, q_2, \ldots q_n), \; i = 1 \text{ to } n,$$

and $q_i(t) = q_i(t_0) + \int_{t_0}^{t} f_i(\lambda)d\lambda, \; i = 1 \text{ to } n.$

Multiport inertances, or *I-fields*, are written  ,

and characterized by

$$f_i = \Phi_i(p_1, p_2, \ldots p_n), \; i = 1 \text{ to } n,$$

and $$p_i(t) = p_i(t_0) + \int_{t_0}^{t} e_i(\lambda)d\lambda, \; i = 1 \text{ to } n.$$

If a *C*-field or *I*-field is to have an associated "energy" state function then certain integrability conditions must be met by the Φ_i functions. In multiport terms the relations given in the foregoing are sufficient to define a *C*-field and *I*-field, respectively.

Mixed multiport storage fields can arise when both *C* and *I*-type storage effects are present simultaneously. The symbol for such an element consists of a set of *C*'s and *I*'s with appropriate ports indicated.

For example, 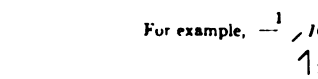 indicates the existence of a set

of relations

$$f_1 = \Phi_1(p_1, q_2, p_3),$$

$$e_2 = \Phi_2(p_1, q_2, p_3),$$

$$f_3 = \Phi_3(p_1, q_2, p_3),$$

and

$$p_1(t) = p_1(t_0) + \int_{t_0}^{t} e_1(\lambda)d\lambda,$$

$$q_2(t) = q_2(t_0) + \int_{t_0}^{t} f_2(\lambda)d\lambda,$$

$$p_3(t) = p_3(t_0) + \int_{t_0}^{t} e_3(\lambda)d\lambda.$$

Multiport dissipators, or *R*-fields, are written 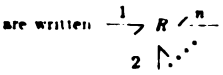

and are characterized by

$$\Phi_i(e_1, f_1, e_2, f_2, \ldots e_n, f_n) = 0, \; i = 1 \text{ to } n.$$

If the *R*-field is to represent pure dissipation, then the power function associated with the *R*-field must be positive definite.

Multiport junctions include 0 junctions and 1 - junctions with *n* ports, $n \geq 2$. The general case for each junction is given in the following.

$e_1 = e_2 = \ldots = e_n$

$$\sum_{i=1}^{n} f_i = 0$$

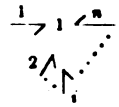

$f_1 = f_2 = \ldots = f_n$

$$\sum_{i=1}^{n} e_i = 0$$

Modulated 2-Port Junctions. The *modulated transformer*, or *MTF* written  implies the realtions

$$e_1 = m(x) \cdot e_2$$

and $$m(x) \cdot f_1 = f_2,$$

where $m(x)$ is a function of a set of variables, *x*. The modulated transformer preserves power; i.e., $P_1(t) = P_2(t)$.

The *modulated gyrator*, or *MGY*, written 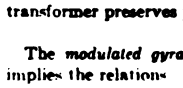 implies the relations

$$e_1 = r(x) \cdot f_2$$

and $$e_2 = r(x) \cdot f_1,$$

where $r(x)$ is a function of set of variables, *x*. The modulated gyrator preserves power; i.e., $P_1(t) = P_2(t)$.

Junction Structure. The *junction structure* of a bond graph is the set of all 0, 1, *GY*, and *TF* elements and their bonds and ports. The junction structure is an *n*-port that preserves power (i.e., the *net* power in is zero). The junction structure may be modulated (if it contains any *MGY*'s or *MTF*'s) or unmodulated.

For example, the junction structure of the graph in Fig. 2(*b*) is a 4-port element with ports 1, 2, 5, and 6 and bonds 3 and 4. It contains the elements 0, *TF*, and 1.

Physical Interpretations

The physical interpretations given in this section are very succinctly stated. References [1], [2], and [3] contain extensive descriptions of physical applications and the interested reader is encouraged to consult them.

Mechanical Translation. To represent mechanical translational phenomena we may make the following variable associations:

1 *effort*, *e*, is interpreted as *force;*
2 *flow*, *f*, is interpreted as *velocity;*
3 momentum, *p*, is interpreted as impulse-momentum;
4 displacement, *q*, is interpreted as mechanical displacement.

Then the basic bond graph elements have the following interpretations:

1 source of effort, *SE*, is a force source;
2 source of flow, *SF*, is a velocity source (or may be thought of as a geometric constraint);

3 resistance, R, represents friction and other mechanical loss mechanisms;

4 capacitance, C, represents potential or elastic energy storage effects (or spring-like behavior);

5 inertance, I, represents kinetic energy storage (or mass effects);

6 transformer, TF, represents linear lever or linkage action (motion restricted to small angles);

7 gyrator, GY, represents gryational coupling or interaction between two ports;

8 0-junction represents a common force coupling among the several incident ports (or among the ports of the system bonded to the 0-junction); and

9 1-junction represents a common velocity constraint among the several incident ports (or among the ports of the system bonded to the 1-junction).

The extension of the interpretation to rotational mechanics is a natural one. It is based on the following associations:

1 effort, e, is associated with torque; and

2 flow, f, is associated with angular velocity.

Because the development is so similar to the one for translational mechanics it will not be repeated here.

Electrical Networks. In electrical networks the key step is to interpret a port as a terminal-pair. Then variable associations may be made as follows:

1 *effort*, e, is interpreted as *voltage*;

2 *flow*, f, is interpreted as *current*;

3 momentum, p, is interpreted as flux linkage;

4 displacement, q, is interpreted as charge.

The basic bond graph elements have the following interpretations:

1 source of effort, SE, is a voltage source;

2 source of flow, SF, is a current source;

3 resistance, R, represents electrical resistance;

4 capacitance, C, represents capacitance effect (stored electric energy);

5 inertance, I, represents inductance (stored magnetic energy);

6 transformer, TF, represents ideal transformer coupling;

7 gyrator, GY, represents gyrational coupling;

8 0-junction represents a parallel connection of ports (common voltage across the terminal pairs); and

9 1-junction represents a series connection of ports (common current through the terminal pairs).

Hydraulic Circuits. For fluid systems in which the significant fluid power is given as the product of pressure times volume flow, the following variable associations are useful:

1 *effort*, e, is interpreted as *pressure*;

2 *flow*, f, is interpreted as *volume flow*;

3 momentum, p, is interpreted as pressure-momentum;

4 displacement, q, is interpreted as volume.

The basic bond graph elements have the following interpretations:

1 source of effort, SE, is a pressure source;

2 source of flow, SF, is a volume flow source;

3 resistance, R, represents loss effects (e.g., due to leakage, valves, orifices, etc.);

4 capacitance, C, represents accumulation or tank-like effects (head storage);

5 inertance, I, represents slug-flow inertia effects;

6 0-junction represents a set of ports having a common pressure (e.g., a pipe tee);

7 1-junction represents a set of ports having a common volume flow (i.e., series).

Other Interpretations. This brief listing of physical interpretations of bond graph elements is restricted to the simplest, most direct, applications. Such applications came first by virtue of historical development, and they are a natural point of departure for most classically trained scientists and engineers. As references [1–4] and the special issue collection in the JOURNAL OF DYNAMIC SYSTEMS, MEASUREMENT, AND CONTROL, TRANS. ASME, Sept. 1972, indicate, bond graph elements can be used to describe an amazingly rich variety of complex dynamic systems. The limits of applicability are not bound by energy and power in the sense of physics; they include any areas in which there exist useful analogous quantities to energy.

Concluding Remarks

In this brief definition of the bond graph language two important concepts have been omitted. The first is the concept of *bond activation*, in which one of the two power variables is suppressed, producing a pure signal coupling in place of the bond. This is very useful modeling device in active systems. Further discussion of activation will be found in reference [3], section 2.4, as well as in references [1] and [2].

Another concept omitted from discussion in this definitional paper is that of *operational causality*. It is by means of causality operations applied to bond graphs that the algebraic and differential relations implied by the graph and its elements may be organized and reduced to state-space form in a systematic manner. Extensive discussion of causality will be found in reference [3], section 3.4 and chapter 5. Systematic formulation of relations is presented in reference [6].

References

1 Paynter, H. M., *Analysis and Design of Engineering Systems*, M.I.T. Press, 1961.

2 Karnopp, D. C., and Rosenberg, R. C., *Analysis and Simulation of Multiport Systems*, M.I.T. Press, 1968.

3 Karnopp, D. C., and Rosenberg, R. C., "System Dynamics: A Unified Approach," Division of Engineering Research, College of Engineering, Michigan State University, East Lansing, Mich., 1971.

4 Takahaski, Y., Rabins, M., and Auslander, D., *Control*, Addison-Wesley, Reading, Ma., 1970 (see chapter 6 in particular).

5 Rosenberg, R. C., "ENPORT User's Guide," Division of Engineering Research, College of Engineering, Michigan State University, East Lansing, Mich., 1972.

6 Rosenberg, R. C., "State-Space Formulation for Bond Graph Models of Multiport Systems," JOURNAL OF DYNAMIC SYSTEMS, MEASUREMENT, AND CONTROL, TRANS. ASME, Series G, Vol. 93, No. 1, Mar. 1971, pp. 35-40.